



Pd/In-based catalysts for nitrate catalytic removal from water: synthesis designs aiming for better N₂ selectivity

Nicolas Alejandro Sacco ^{a,†}, Fernanda Miranda Zoppas ^{a,*†}, Vanina Aghemo^a, Thiago Beltrame^b and Fernanda Albana Marchesini^a

^a Instituto de Investigaciones en Catálisis y Petroquímica (INCAPE-CONICET), Santiago del Estero 2829, Santa Fe, Argentina

^b Laboratório de Corrosão, Proteção e Reciclagem de Materiais LACOR-UFRGS (Universidade Federal do Rio Grande do Sul), Av. Bento Gonçalves, 9500, Porto Alegre, RS, Brazil

*Corresponding author. E-mail: fzoppas@fiq.unl.edu.ar

[†]These authors contributed equally to the manuscript production.

 NAS, 0000-0003-3999-3073; FMZ, 0000-0002-7747-2183

ABSTRACT

Catalysts based on Pd/In were prepared through the wet impregnation method using Al₂O₃, SiO₂, and TiO₂ as supports. The impact of the synthesis procedure on N₂ selectivity was studied. Characterization was performed using X-ray fluorescence and scanning electron microscopy–energy dispersive spectroscopy analysis. The catalytic performance of these materials was evaluated for nitrate removal from water in a batch reactor. The order of better nitrate removal was found to be Al₂O₃>TiO₂>SiO₂. The selectivity towards N₂ was also impacted by the support used, with Al₂O₃-based catalysts being the most selective and TiO₂-based the least due to strong metal–support interaction. The synthesis stages also impacted nitrate removal efficiency and selectivity, with the highest N₂ selectivity (94.4% at 90% nitrate conversion) found in catalysts where In was added after Pd and underwent intermediate calcination, reduction and final reduction stages.

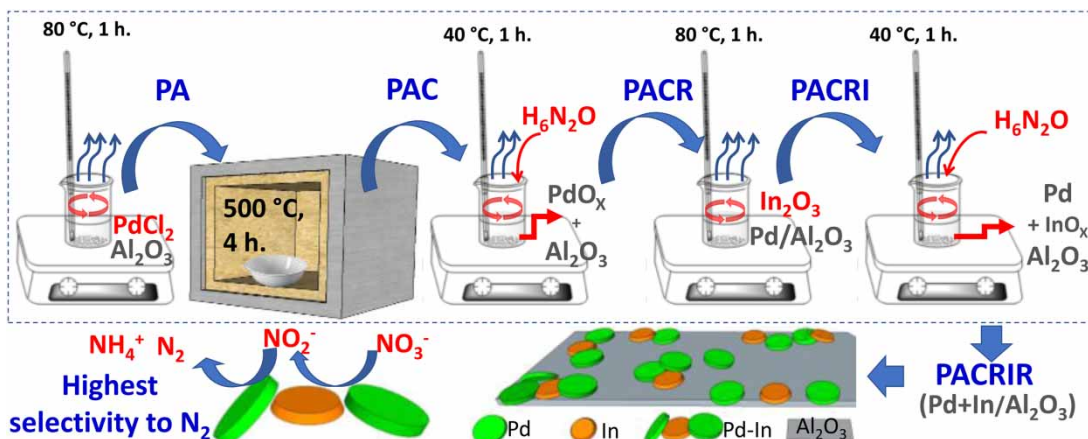
Key words: catalytic nitrate removal, Pd–In/Al₂O₃, Pd–In catalysts, Pd–In/SiO₂, Pd–In/TiO₂ synthesis design

HIGHLIGHTS

- Pd,In-based catalysts were prepared on different supports by varying sequential synthesis steps aiming for higher N₂ selectivity in nitrate reduction.
- Total nitrate conversion was obtained using Pd,In/Al₂O₃ and Pd,In/TiO₂.
- The catalytic performance was influenced by the support used in the synthesis.
- Pd,In/Al₂O₃ was the most selective to N₂.
- PACRIR synthesis was the most suitable for the catalytic removal of nitrate from water.

This is an Open Access article distributed under the terms of the Creative Commons Attribution Licence (CC BY 4.0), which permits copying, adaptation and redistribution, provided the original work is properly cited (<http://creativecommons.org/licenses/by/4.0/>).

GRAPHICAL ABSTRACT



1. INTRODUCTION

Providing high-quality drinking water is one of the Sustainable Development Goals (SDGs) for 2030 established by the United Nations General Assembly in 2015. Despite this, water-body pollution constitutes one of the areas of major concern for research. The pollution of groundwater and surface water caused by nitrate has become a serious problem since about 90% of the world's drinking water supplies come from groundwater sources (Ramalingam & Subramania 2021), and due to the hazard it represents to human health and the environment (Kiani *et al.* 2022; Qasemi *et al.* 2022; Singh *et al.* 2022). Nowadays, according to the United Nations (UN) report (UNESCO 2019), nitrate is the most common chemical contaminant found in groundwater and the most widespread pollutant in groundwater due to its high solubility in water and the difficulty of fixing it in the soil. There is an increasing concern about this pollutant as a consequence of intensive anthropogenic activities, which are known as the main source of this pollutant. The excessive use of fertilizers and the discharge of liquid industrial waste without appropriate treatment represent the major fonts of nitrate pollution in groundwaters (Chauhan & Srivastava 2021).

High concentrations of nitrates may damage the quality of water resources and have significant adverse effects on human health, like methemoglobinemia (blue baby syndrome) as well as cancer and hypertension caused by the metabolic conversion of nitrite into N-nitroso compounds (Clark *et al.* 2020). In this sense, the removal of nitrates from water bodies is necessary to ensure the consumption of clean and safe drinking water.

Numerous methods have been reported for the removal of nitrates from water involving adsorption (Wang *et al.* 2021; Liu *et al.* 2022), reverse osmosis (Fuentes & Hwang 2021; Scholes *et al.* 2021), biological denitrification (Hurtado-Martinez *et al.* 2021; Pang & Wang 2021), electrochemical reduction (Fu *et al.* 2021; Fu *et al.* 2022), and catalytic reduction (Martínez *et al.* 2017; Guo *et al.* 2018; Lv *et al.* 2022). Among them, catalytic nitrate reduction from water has been proposed as an efficient and inexpensive method for meeting NO_3^- and NO_2^- standards and removing nitrate. It has also advantages such as no sludge production, low energy consumption, and high N_2 selectivity (Martínez *et al.* 2017; Tokazhanov *et al.* 2020).

For catalytic nitrate removal, it is critical to synthesize a catalyst with suitable metals and structures to obtain a good nitrate removal capacity. The catalytic composition, structure, and supports not only affect the reaction but also the reaction rate and the end-products (Shen *et al.* 2021). Bimetallic catalysts have been proven to be more efficient than monometallic catalysts in terms of conversion and selectivity to nitrogen gas in the catalytic denitrification of water (Shen *et al.* 2021). Sá & Vinek (2005) studied the catalytic hydrogenation of nitrate over a bimetallic Pd/Cu catalyst and compared its catalytic performance with the corresponding monometallic catalysts (Pd and Cu). The authors found that monometallic Pd catalysts could reduce NO_3^- , but its degradation was very slow. The monometallic Cu catalyst was only active at the beginning of the reaction, and the fast oxidation of Cu led to the deactivation of the catalyst, Pd being necessary to stabilize Cu in its lower oxidation state. On the other hand, Pd/Cu was demonstrated to be more efficient than Pd and Cu monometallic catalysts, and a better activity and selectivity in nitrate degradation was achieved by reducing the amount of the noble metal of Pd/Cu from 5 to 2 wt.%. Devadas *et al.* (2011) studied catalytic nitrate reduction using Pd/CeO₂ and PdSn/CeO₂ catalysts and found that although

Pd/CeO₂ is more active than the bimetallic catalysts under pure hydrogen flow, the monometallic Pd/CeO₂ is inactive for nitrate reduction in the presence of CO₂. The bimetallic catalysts turn out to be more active than under pure hydrogen flow and also than the monometallic catalyst with a low selectivity toward ammonium ions, which are the undesired product of the reaction. Thus, the Pd-Sn/CeO₂ catalyst is comparatively the most suitable catalyst for nitrate reduction. One explanation for the monometallic Pd/CeO₂ activity was given by [Devadas *et al.* \(2011\)](#), who investigated the performance of Pd/CeO₂ and reported that after reduction under hydrogen flow, Ce was in its low coordination form and vacancies of oxygen were created on the surface. Such reducible supports were capable of allowing nitrate to initiate the reduction reaction, but the main product of the reaction was ammonium due to the high availability of electrons to over-reduce NO(ads) – NO adsorbed in active sites.

In most of the reported works, the catalysts used in catalytic denitrification were composed of a combination of noble metals, usually Pd, Pt, or Rh, and promoter metals (In, Sn, Cu, Au, and Ni) deposited on different supports ([Imura *et al.* 2014](#); [Li *et al.* 2019](#); [Hamid *et al.* 2020](#)).

Nitrate reduction by bimetallic catalysts involves a multi-step redox process requiring an additional reducing agent, being H₂(g) being the most commonly used ([Werth *et al.* 2021](#)). The role of the transition metal is to reduce nitrate to nitrite by a redox process, leading to its oxidation; and the function of the noble metal is to stabilize the transition metal in its lower oxidation state by hydrogen spillover to prevent deactivation. This is the reason why bimetallic catalysts are more efficient than monometallic ones ([Santos *et al.* 2020](#)).

It is known that the characteristics of the support material and also the properties of the metal particles can influence the catalytic performance of bimetallic catalysts in the elimination of nitrates. The properties include morphology, porosity, and surface area, among others ([Tokazhanov *et al.* 2020](#)). [Soares *et al.* \(2011\)](#) studied the influence of the support (TiO₂, CeO₂, composite of activated carbon and CeO₂, and activated carbon and Mn) in the performance of Pd monometallic and Pd-Cu bimetallic catalyst for the reduction of nitrate in water and found that supports play a key role in the catalytic performance and, in some cases, are involved in the reaction mechanism. For these catalysts, it was found that the Brunauer–Emmett–Teller (BET) surface area does not have a significant effect on the catalytic activity, once catalysts with different surface areas have a similar nitrate conversion. In the catalyst supported on TiO₂, the selectivity to nitrogen decreased with conversion, which was attributed to the high hydrogenation capacity of this type of catalyst, producing a higher amount of ammonium. Pd-Sn bimetallic catalysts were supported on four zeolites with different degrees of crystallinity, morphology, BET surface area, and pore volume, and their catalytic performance in nitrate reduction was compared ([Park *et al.* 2019](#)). The authors attributed the better nitrate removal and N₂ selectivity to the high surface area and stability of zeolite phases. The effect of promoter metal and catalytic loading on Pd-In and Pd-Sn bimetallic systems were studied by [Sanchis *et al.* \(2021\)](#). The authors found that the Pd:promoter weight ratio and the order of impregnation on alumina, and the nature of the promoter influence both the activity and selectivity of the bimetallic systems. The reduction mechanism followed the next three steps represented by Equations (1)–(3), and the mechanism is added in the Supplementary Material. In Pd:In bimetallic catalysts, the In particles reduced nitrate to nitrite according to the reaction as shown in Equation (1). After that, nitrite diffused to closer Pd sites to be reduced to N₂ or NH₄⁺ (Equations (2) and (3), respectively), depending on intrinsic characteristics of the catalysts and environmental conditions. Those properties acted synergistically, producing hydrogen adatoms (adsorbed atomically over the surface due to spillover ([Clark *et al.* 2020](#))), which were responsible for regenerating the oxidized In sites and providing H to reduce the nitrate according to the reaction described above.



In this sense, metal disposition, interactions between metal–metal and metal–support, metal loading, atomic configuration, and size had a significant effect on the reduction rate of nitrate ([Guo *et al.* 2018](#)). Moreover, the co-production of ammonium during nitrate reduction is still the main drawback of the process when the aim is to obtain drinking water, as it causes adverse effects, such as toxicity, to some aquatic organisms in surface waters, increasing the need for disinfectants and/or biological nitrification in water distribution systems ([Garcia-Segura *et al.* 2018](#)). Even so, there is a lack of information on

synthesizing materials that are both efficient in removing nitrate from water and highly selective for N_2 . In this line, it is important to remark that *Yin et al. (2018)* showed that this bimetallic catalyst could be used in the catalytic reduction of oxy-anions such as chromium, chlorine, and bromine as examples. Although this implementation is not the goal of the present study, it is possible to think of a practical, wide implementation of the material, which will give it the highest added economic value.

In this work, (Pd, In)-based catalysts deposited by the wet impregnation method onto different supports, alumina (Al_2O_3), silica (SiO_2), and titania (TiO_2) were prepared and evaluated for nitrate removal from water to study the influence of support on the catalytic performance and selectivity. Then, catalysts with the same formulation were synthesized by alternating the sequential steps of synthesis, including both the order of deposition of the noble and promoter metals on the support, as well as the calcination and reduction stages, to study how that affects the properties of the catalytic systems and to find the one that allows the highest selectivity to N_2 . Thus, this study aims to determine whether the type of support used during the synthesis or the sequence of synthesis steps has a significant influence on the catalytic properties of the bimetallic system for the catalytic removal of nitrate from water and to report the conditions that allow obtaining a catalyst with high activity toward the removal of nitrate from water and high N_2 selectivity. Thus, it would be possible to attain a safer and more reliable water supply in the future by treating nitrate-contaminated water with high N_2 selectivity.

2. EXPERIMENTAL

2.1. Reagents

Gamma- Al_2O_3 (KEDJEN CK300, 180 m^2/g , vol. pore 0.5 cm^3/g), SiO_2 (Alfa Aesar 300 m^2/g , vol. pore 1 cm^3/g), and TiO_2 (Degussa, P25, 48 m^2/g , pore 0.28 cm^3/g) were used as support for the synthesis of the (Pd, In)-based catalysts. These oxides with well-differentiated acid properties, in terms of their surface sites and acid strength, were selected as supports for the catalysts' conformation to evaluate their influence on the physicochemical and catalytic properties.

$PdCl_2$ (Sigma Aldrich, p.a.), $In_2O_3 \cdot 3H_2O$ (Sigma Aldrich, 99.9%) were employed as precursors for metallic Pd and In, respectively. Hydrazine chloride (Sigma Aldrich, p.a.) was used as the reducing agent for the synthesis. KNO_3 (Cicarelli, p.a.) and hydrogen gas (INDURA, 99.998%) were employed as the nitrate precursor and the reducing agent, respectively, for the catalytic assays. HCl (Cicarelli p.a., 37%) was used in the analytical determination of products and reactants.

2.2. Catalyst preparation

The catalysts were prepared by combining 1 wt.% palladium and 0.25 wt.% indium. This metallic proportion has been studied in previous works and was chosen due to its high activity for nitrate removal from water (*Marchesini et al. 2008a, 2012; Zoppas et al. 2018*). Generally, the preparation of catalysts reported in the above-mentioned works was carried out by the wet impregnation method and consisted of the following steps: (1) Pd and In precursor solutions were mixed with the support, (2) the mixed solution was stirred at 80 °C until total evaporation of the liquid phase, (3) the solid mixture was dried at 80 °C for 12 h in an oven and (4) calcined at 500 °C for 4 h at a heating rate of 10 °C/min, and finally (5) the catalyst was reduced in hydrazine 0.8 M at 40 °C for 1 h. All the catalysts, after reduction, were rinsed five times with deionized water and dried in a vacuum oven at 60 °C for 12 h. In this work, we decided to modify the synthesis step sequence to study its influence on the properties of the catalysts, so we developed five synthesis sequences from which we obtained the following catalysts: PSCRIR, PSCRI, PISCR, PSCIR, and PSCICR. The catalysts were named according to the order of synthesis steps. The letters represent the following components (P, I, S) and processes (C, R): P: palladium; I: indium; S: support; C: calcination at 500 °C at 10 °C/min; R: reduction with hydrazine hydrate solution (0.8 M) at 45 °C. The synthesis sequence for each one is described below and illustrated in [Figure 1](#).

2.2.1. PSCRIR synthesis

PSCRIR catalyst was prepared as follows: (1) wet impregnation of Pd over the supporting material and (2) calcination at 500 °C for 4 h. In this step, Pd oxides were obtained on the surface of the catalyst. (3) Reduction of the material with hydrazine hydrate solution 0.8 M to obtain Pd^0 (metallic form). (4) Wet impregnation of In precursor onto the material obtained in step 3. (5) Reduction of the catalyst obtained in hydrazine hydrate solution. Then, upon reduction in the aqueous phase, Pd was reduced by the action of hydrazine, forming strongly anchored Pd^0 .

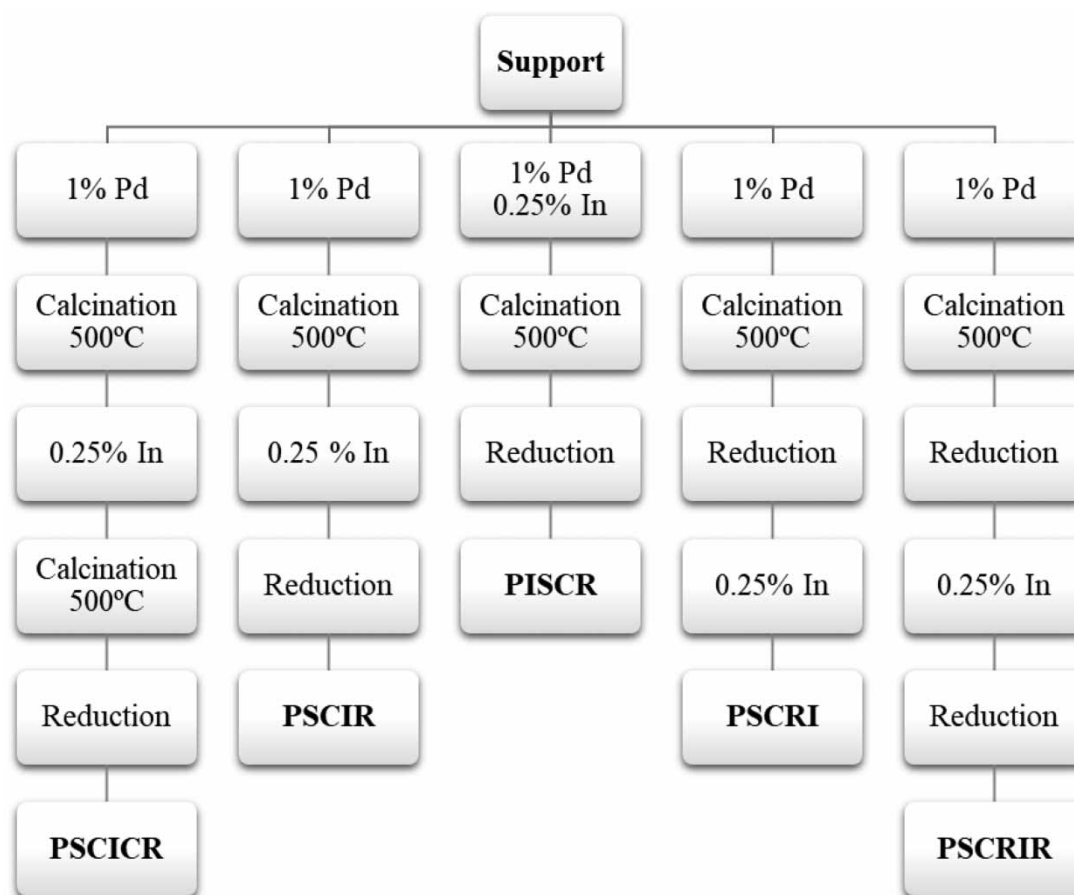


Figure 1 | Scheme of the steps carried out in the synthesis of each catalyst with the supports. The letters represent P: palladium; I: indium; S: support (specified in the work with the letters alumina (A), silica (S), and titania (T)); C: calcination at 500 °C; R: reduction with N_2H_4 solution 0.8 M at 45 °C.

2.2.2. PSCRI synthesis

PSCRI catalyst was synthesized as follows: (1) wet impregnation of the Pd precursor onto the support. (2) Calcination at 500 °C for 4 h, obtaining Pd oxides on the surface of the support. (3) Reduction of the material with hydrazine hydrate solution 0.8 M leading to the formation of Pd^0 . (4) Wet impregnation with the indium precursor onto the material obtained after step 3.

In the PSCRI catalyst, palladium was calcined on the support and then reduced, generating isolated metallic species on the support. Indium was then added, allowing its deposition on the surface of the metallic palladium.

2.2.3. PISCR synthesis

The following is a description of the steps followed for the synthesis of PISCR catalyst: (1) wet impregnation of Pd and In precursors. (2) Calcination at 500 °C for 4 h. After calcination, it was expected to obtain the material surface coated with Pd oxides and In oxides, anchored to the support. (3) Reduction with hydrazine hydrate solution 0.8 M.

2.2.4. PSCIR synthesis

PSCIR catalyst was prepared as follows: (1) wet impregnation of Pd precursors onto the support. (2) Calcination at 500 °C for 4 h. (3) Wet impregnation of In precursors. (4) Reduction in hydrazine hydrate solution 0.8 M. In PSCIR, the palladium was anchored to the support by the calcination process, and the indium was deposited randomly on the catalyst surface.

2.2.5. PSCICR synthesis

For PSCICR synthesis, we proceeded as follows: (1) wet impregnation of Pd precursors onto the support. (2) Calcination at 500 °C for 4 h. (3) Wet impregnation of In precursors. (4) Calcination at 500 °C for 4 h. (5) Reduction in hydrazine hydrate solution 0.8 M.

2.3. Characterization

2.3.1. Scanning electron microscopy

Scanning electron microscopic (SEM) micrographs and EDX spectra were obtained with a Carl Zeiss Sigma microscope. Moreover, a JEOL scanning electron microscope model JSM 35C was used to elucidate the composition and distribution of Pd and In over the supports (SEM-EDS).

2.3.2. X-ray fluorescence

The elemental quantification of elemental Pd and In was carried out by employing a Shimadzu spectrometer, equipped with an energy-dispersive analytical system (EDX-720) with a high detection range (from Na11 to U92), a rhodium X-ray source, operated at 50 kV and 100 μ A, using five X-ray primary filters.

2.4. Catalytic tests

The catalytic performance of the Pd–In catalysts on the nitrate reduction was performed in a 250 mL batch reactor with a catalyst concentration of 2.5 g/L. The reactor was placed on a magnetic stirring system (~800 rpm) to reduce the mass transfer limitations. The reaction system was maintained under atmospheric pressure at room temperature using a thermostatic bath at 25 °C. For catalytic evaluation, as described in Figure 2, the following procedure was followed: 80.0 mL of deionized water was added to the reactor, and N₂ was injected for at least 20 min, to purge atmospheric CO₂ and O₂. Then, the catalyst was added to the aqueous medium, and H₂ was bubbled. After 20 min, a KNO₃ solution was added to reach 100 ppm of N-NO₃ in the reaction medium (concentrations similar to those found in water treatment concentrates), this moment being considered as the initial time ($t = 0$ min). The pH was controlled by a TPX1 pH meter (Hanna Instruments) and maintained at 5 using an HCl solution of 0.1 M. The reaction was monitored for 120 min, taking aliquots of the reaction medium at fixed time intervals in order to quantify the production of nitrite and ammonium.

2.5. Analytical methods

The ion concentration in the solution was determined using a UV–Vis spectrophotometer (Cole Parmer 1100). To analyze nitrate, the Cd column reduction method was used, followed by the Griess method (absorbance at 543 nm) (APHA/AWWA/WEF 2017). The Griess method was also used to read the nitrite, and finally, the modified Berthelot method was used for ammonium determination (absorbance at 633 nm) (Searle 1984). The conversion (X) and the selectivity (S) to N₂ were calculated according to Equations (4) and (5), respectively:

$$X(\%) = \left[1 - \left(\frac{C}{C_0} \right) \right] \times 100 \quad (4)$$

$$S(\%) = \left[\frac{C_A}{(C_0 - C)} \right] \times 100 \quad (5)$$

C_0 is N-ppm of nitrates at the beginning of the reduction process, C is N-ppm of nitrates at time t , and C_A is the concentration of N-ppm products (nitrites or ammonia) at time t .

The initial rate (v_i , given in ppm/min) was estimated taking into account that up to 10% conversion, the system was not yet affected by its reaction products. Therefore, v_i was calculated as the slope of the nitrate concentration as a function of the time curve at the time at which 10% of nitrate was converted (the time when the concentration of N-NO₃ in the reactor was 90 ppm).

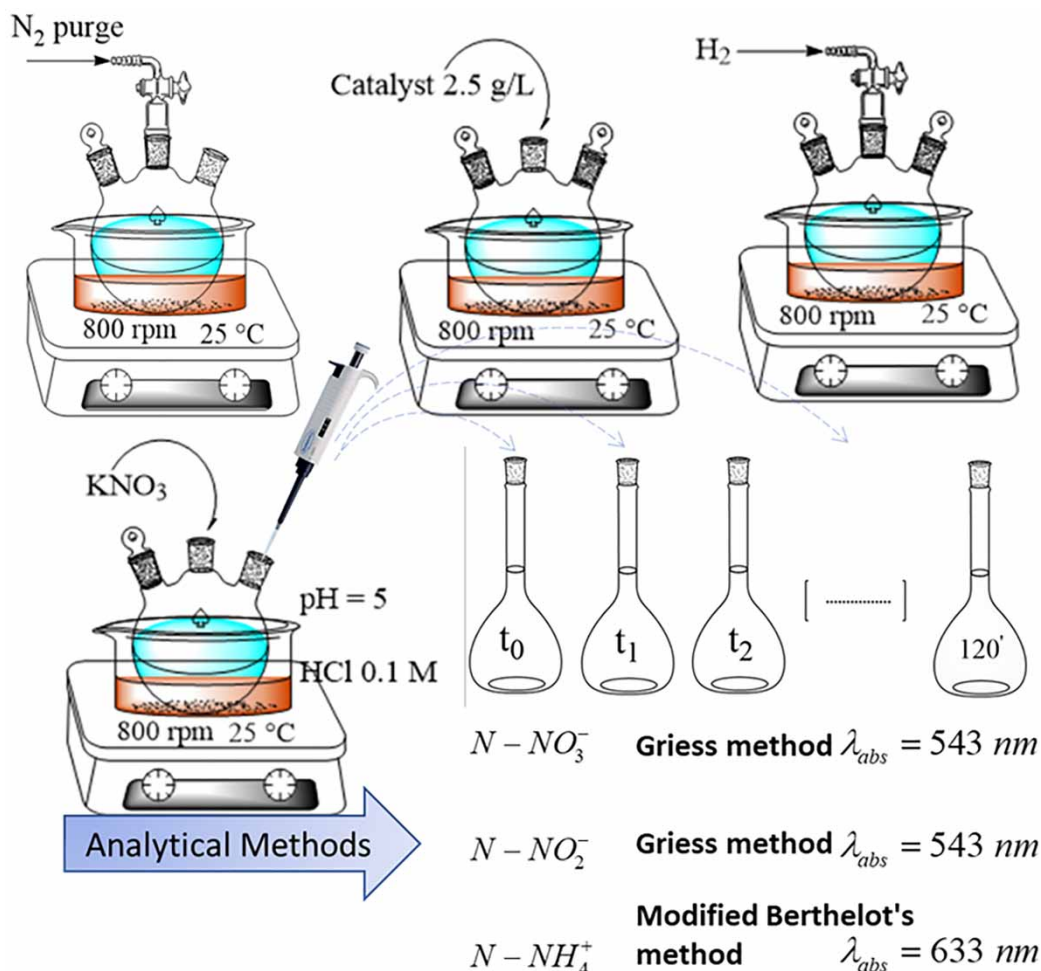


Figure 2 | Reaction scheme and methods used for the quantification of the ions of interest.

3. RESULTS AND DISCUSSION

3.1. Catalyst characterization

Pd and In atomic percentages, obtained by X-ray fluorescence (XRF), are summarized in Table 1. The Pd and In retention percentages were estimated taking into account the amount added in the synthesis procedure and the values obtained by XRF. A composition deviation from the theoretical values was observed after each synthesis procedure. The highest retained metal percentage was observed in samples supported on TiO_2 (85%–99%). Regarding SiO_2 - and Al_2O_3 -based catalysts, when calcination occurs after impregnation, the greater proportion of Pd and In was retained by the support for PIACR (49%) and PISCR (46%). It is believed that due to the lower interaction with Al_2O_3 and SiO_2 , it is only possible to promote the anchoring of both metals at the support surface with a calcination step after the impregnation. This affirmation is corroborated by Wang *et al.* (2021), who calculated the adsorption energy of each of the Pd nanoparticles (NPs) over Al_2O_3 , SiO_2 , and TiO_2 and showed that a higher interaction occurred with TiO_2 . Concerning TiO_2 support-based catalysts, the higher retention occurs when In was impregnated after Pd calcination and reduction (PTCRIR and PTCRI). Then, Pd reacted producing a strong metal–support interaction (SMSI) (Jia *et al.* 2017) with titania terminal OH and, after reduction, the reduced Pd reacted selectively with In, resulting in a stable bimetallic particle of Pd:In. This type of metal–support interaction (MSI) produced by the sequential method of preparation was recognized through the decrease in the capability to chemisorb molecules, minimizing the metal nanoparticles' superficial energy and consequently blocking the accessibility to H_2 to react dissociatively with the Pd particles (Lou *et al.* 2020). Chen *et al.* (2017) reported that the nitrogen-doping TiO_2 enhanced the MSI of the Pd– TiO_2 system due to an electronic promoting effect. In this work, hydrazine hydrate was used for the reduction

Table 1 | Pd and In content (wt.%) obtained by XRF in the Pd:In catalysts

Catalyst	wt.% (XRF)		Retention	
	Pd	In	%Pd	%In
PACIR	0.45 ± 0.01	0.06 ± 0.01	45	24
PACRIR	0.40 ± 0.03	0.07 ± 0.02	40	28
PIACR	0.49 ± 0.05	0.06 ± 0.01	49	24
PACRI	0.41 ± 0.01	0.06 ± 0.01	41	24
PACICR	0.41 ± 0.04	0.08 ± 0.02	41	32
PTCIR	0.85 ± 0.07	0.19 ± 0.02	85	76
PTCRIR	0.91 ± 0.08	0.13 ± 0.02	91	52
PITCR	0.86 ± 0.06	0.25 ± 0.01	86	100
PTCRI	0.99 ± 0.02	0.15 ± 0.01	100	60
PTCICR	0.90 ± 0.06	0.15 ± 0.02	90	60
PSCIR	0.40 ± 0.03	0.08 ± 0.01	40	32
PSCRIR	0.32 ± 0.02	0.10 ± 0.01	32	40
PISCR	0.46 ± 0.04	0.08 ± 0.01	46	32
PSCRI	0.37 ± 0.06	0.05 ± 0.01	37	20
PSCICR	0.37 ± 0.08	0.06 ± 0.01	37	24

P, Pd; I, In; A, alumina support; S, silica support; T, titania support; C, calcination step; R, reduction step.

PdO_x, and this reagent could interact with the acidic sites of the support (Wojcieszak *et al.* 2013) and remain on it providing N-doping TiO₂ support which would enhance the MSI with Pd particles. On the other hand, the higher retention of In in the catalysts supported on TiO₂, compared with the other two supports, suggested a preferential deposit of In on Pd during synthesis, and it could be associated with a lower MSI concerning Pd when SiO₂ and Al₂O₃ were used. This process is thermodynamically favored considering the possible redox mechanism. Metallic Pd can react with In(III) and this ion is reduced to In(0) over Pd. Then, the metallic form of the novel metal was reloaded in the next step with the reduction of H₂. Thus, In was deposited over Pd, and Pd had an electronic effect over In, and at a low wt.% In remained reduced over Pd (Guo *et al.* 2018). This process resulted in a bimetallic particle, bonded by the most stable energetic position and electrostatic forces, and leach resistant. Although energetic calculus is necessary to corroborate what we can appreciate experimentally due to the low lixiviation, the affirmation is supported by Wang *et al.* (2021), who calculated the adsorption energy of each of the Pd NPs over Al₂O₃, SiO₂, and TiO₂ and showed that a higher interaction occurred with TiO₂. Since, in this study, the temperature effect was only introduced by the calcination process, and the reduction stage occurred in mild conditions, the aggregation of the particles observed over the surface could have resulted as a consequence of the thermal treatment. It is well known that the extent of MSI depends on the nature of the metal but mostly on the size of the particles and the nature of the support (Coq 2000). The support acted as a supramolecular ligand and has been claimed to promote specific electronic properties and/or geometrical features of the nano-sized supported metal particles. The key point lies in the strength of interaction between the d-band of the metal and the molecular orbitals of reactants and products (Coq 2000). Also, electronic interactions between Pd NPs and the TiO₂ support rise by decreasing particle size, as a result, creating more admetals on the Pd NPs in contact with TiO₂ (Zhao *et al.* 2022).

In this sense, the In ability to deposit preferentially over Pd during synthesis was reflected by the higher retention of indium in the catalysts supported on titanium, compared with the other two supports, which presented a lower MSI with respect to Pd. Two situations could produce the preferential deposition and anchoring effect. In the first place, it is known that Al₂O₃ and TiO₂ have a higher density of reactive hydroxyl groups compared with SiO₂ and therefore provide more anchoring sites for Pd and In (Yang & Bent 2017). In the second place, as titanium is a semiconductor support, the availability of electrons to create a chemical interaction between Pd and In is higher than that in the other two isolating supports (alumina and silica). Wang *et al.* (2021) showed that the adsorption energy of a Pd cluster increased in the sequence SiO₂ (0.85 eV) < Al₂O₃ (2.12 eV) < TiO₂ (3.05 eV), which was accompanied by a decrease in the distance between the cluster and the surface.

Those properties may contribute to justify why a more stable Pd cluster is produced on TiO₂, and due to this energy, In is preferentially linked to Pd in this material. No significant differences were observed between SiO₂ and Al₂O₃ in metal retention, in spite of the significant energetic difference, which could be associated with the almost two-fold higher surface area of SiO₂ (300 m²/g). Durkin *et al.* (2018) showed that the ratio of Pd to In measured in different nanoparticle regions was more uniform than the one observed in Pd–Cu catalysts. It was consistent with a uniform distribution, which is compatible with a selective deposition process induced by a reduced Pd or by an electron-rich zone near Pd. It is noteworthy that Pd (2.20 eV) had a higher electronegativity than In (1.78 eV) and that this difference (0.42 eV) favored the formation of a very polar interaction between both elements. The ratio of Pd to In measured in different nanoparticle regions appeared to be more uniform than the one observed in the Pd–Cu catalysts from our previous study, consistent with the XPS and energy-dispersive spectroscopy (EDS) data that showed that the Pd–In composition throughout the fibers was uniform.

Byun *et al.* (2020) found that the active phase/support atomic ratio decreased in a similar order as the ability to retain metal decreased. The lower the active phase/support atomic ratio, the lower the interaction with the support, and a less active phase is retained after the process. The order proposed is Al₂O₃ > TiO₂ > SiO₂.

In this study, the order in the active phase/support atomic ratio was TiO₂ > Al₂O₃ > SiO₂ and was preferably modulated by the sequential synthesis process more than by the MSI. Probably, TiO₂ can retain a higher proportion of metals than the other supports since metals had the strongest interaction with the semiconductor support. Moreover, TiO₂ and interactions are weaker with isolator supports such as SiO₂ and Al₂O₃ (Coq 2000). These findings are in line with several of the aforementioned authors who stated that superficial energy (or the enhanced electron accumulation at the surface) contributed to stabilize the Pd cluster over the support surface depending on its semiconductor properties. Thus, as the TiO₂ had the highest energy, the particles were more established in this surface (Li *et al.* 2022). In addition, Wang *et al.* (2021) confirmed, with optimized geometric configurations of Pd/Support (where the supports are SiO₂, Al₂O₃, TiO₂, and CeO₂), that the adsorption energy increased in this order, suggesting that the strength of the MSI also increased in this order: Pd/SiO₂ < Pd/Al₂O₃ < Pd/TiO₂.

SEM micrographs of some catalysts prepared using silica, titania, and alumina are shown in Figures 3–5, respectively. Figure 3 shows micrographs of the SiO₂ support (Figures 3(A1) and 3(A2)), PSCICR (Figures 3(A3) and 3(A4)), and PSCRIR (Figures 3(A5), 3(A6), and 3(A7)) catalysts at different magnifications. Figure 3(A2) reveals the rough surface of the support. Regarding catalysts (Figure 3(A4) and 3(A7)), it can be seen that the procedure synthesis affects the morphology of the active phases deposited. A higher agglomeration of catalytic particles is observed in the PSCRIR catalyst than in the system through which In, after deposition, was calcined and reduced (PSCICR). As Figure 3(A7) shows, agglomerates of about 1 μm are observed in the PSCRIR catalyst.

A SEM-EDS analysis of PSCIR catalyst (Figures S1 and S2) was carried out to analyze the active phase distribution and quantification. Pd and In wt.% are summarized in Table S1. Pd agglomerates of about 7 μm were distributed heterogeneously over the SiO₂ support, which do not include In on their surface. However, In particles were detected on the support surface in much smaller particles than the Pd agglomerates. In a region containing Pd and In (Figure S2), a weight ratio of Pd/In = 2 was found, a value equal to half the nominal weight ratio, indicating that In particles were highly dispersed onto the silica surface since XRF measurements indicated a Pd/In ratio close to the nominal value.

In Figure 4, micrographs of TiO₂-supported catalysts are shown. In the highest magnification of the micrograph of the support (Figure 4(B2)), a hierarchical aggregated cauliflower-like structure, which is typical of the rutile phase (Shi *et al.* 2019; Ren *et al.* 2022), can be seen. At higher magnifications (Figure 4(B4) and 4(B7)), it can be seen that the particles present a cauliflower-like structure, following the structure of the support (TiO₂).

Through the SEM-EDS map of the PTCRI catalyst (Figure S3 in Supplementary Material), a Pd/In ratio equal to 3 was obtained (Table S1), which was lower than the theoretical value (4). This behavior could be related to the strong interaction of Pd with the support, as seen by XRF, promoting that most Pd is in bulk, and In preferentially on the surface of the catalyst.

Regarding alumina-supported catalysts (see Figure 5), C1–C3 show alumina micrographs, C4–C7 show micrographs of the PACRIR catalyst, and C8–C11 show micrographs of the PIACR catalyst.

Figure 5(C10) reveals the presence of repetitive prism- or conical-like structures, attributed to Pd agglomerates since micrographs of the support do not show this tendency and SEM-EDS analysis has shown a good distribution of In on the support. Also, it is clear from the micrographs C7 and C10 that PIACR maintains a rough surface like the Al₂O₃ support, while PACRIR seems to have smoother surfaces. Moreover, the agglomerates formed in PIACR are much smaller (about

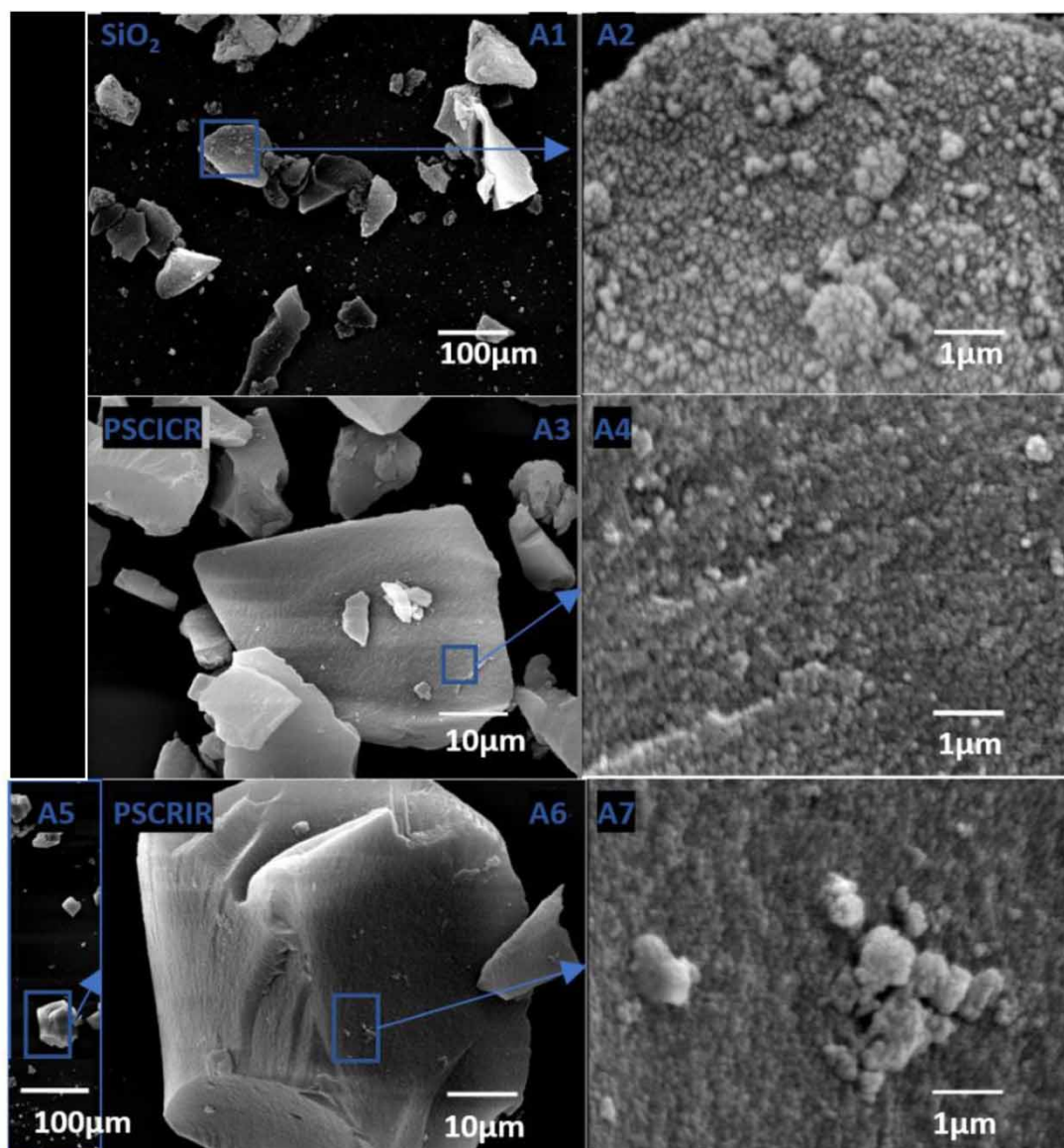


Figure 3 | SEM micrographs of SiO₂ (A1, A2), PSCICR (A3, A4), and PSCRIR (A5–A7).

five times smaller) than those observed in the PACRIR catalyst, in agreement with what was observed by SEM-EDS (Figures S4–S8).

Figures S4–S8 show SEM-EDS analysis of alumina-supported catalysts. Although the Pd/In ratio in these catalysts was lower than nominal, indicating that there was lower retention of Pd with respect to In, the effect of the variation of the synthesis steps was mostly seen in the distribution of the active phases. In the catalysts in which the Pd and In precursors were simultaneously impregnated (PIACR), the atomic distribution of both elements followed the same pattern, indicating the coexistence of both phases in different regions. This would indicate that the introduction of intermediate stages, either calcination or reduction, considerably affected not only the distribution but also the loading of the active material.

However, not only observed was the effect of the order of the synthesis steps on the catalytic loading or distribution of active elements but also the influence of the support on the retention of both Pd and In. As mentioned above and in agreement with the silica-supported catalysts, the Pd and In retention values obtained by XRF in alumina-supported catalysts were lower than those observed for the titania-supported systems.

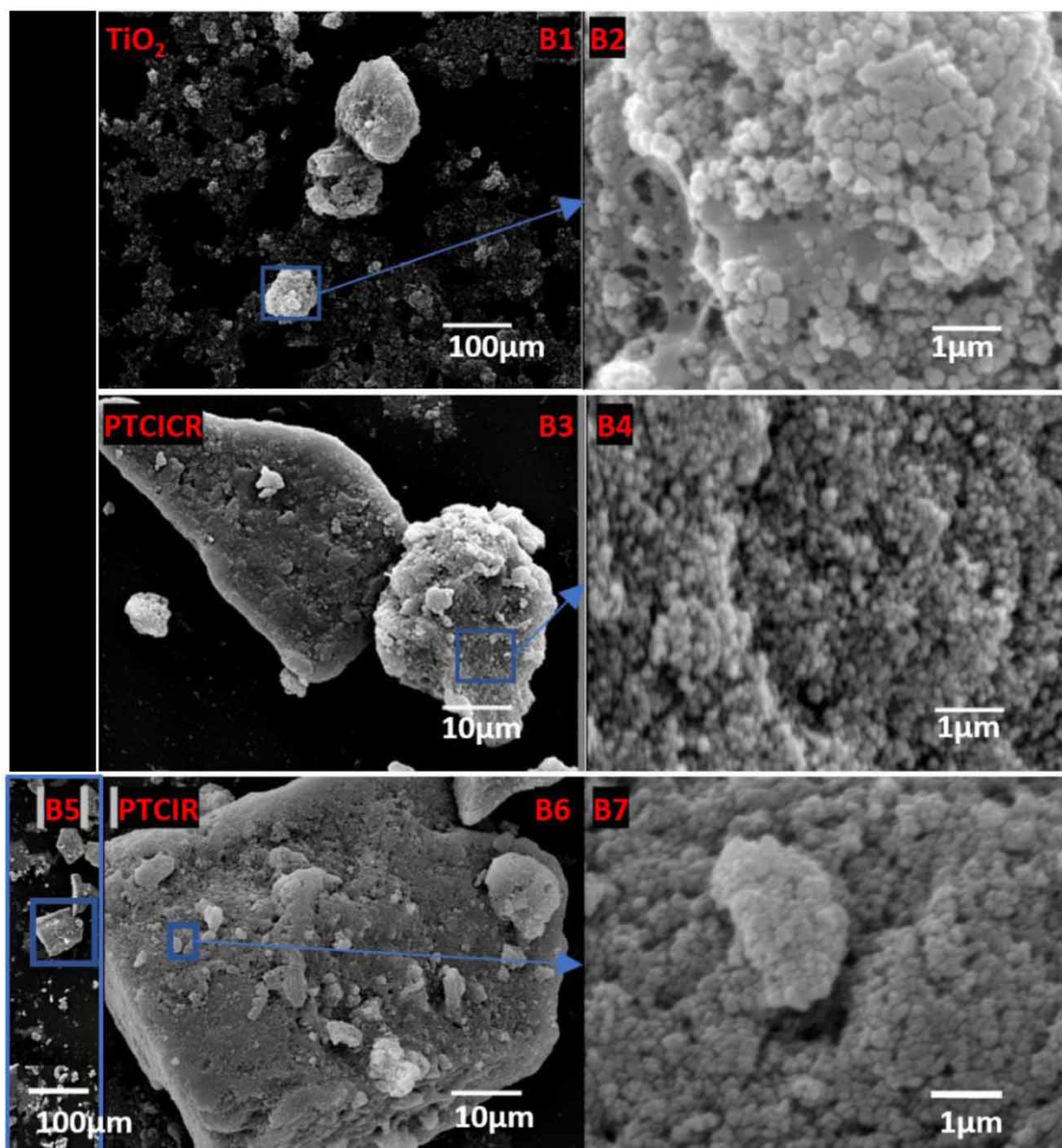


Figure 4 | SEM micrographs of TiO_2 (B1, B2), PTCICR (B3, B4), and PTCIR (B5–B7).

A strong interaction between Pd and In leading to the formation of intermetallic compounds was reported in Pd, In systems supported on Al_2O_3 and SiO_2 (Krawczyk *et al.* 2011). Moreover, in the presence of the intermetallic compound, a decrease in selectivity to nitrogen and, at the same time, an increase in the amount of ammonia formed was observed during the reaction (Witońska *et al.* 2008). On the other hand, it was reported that, for titanium support, an SMSI with noble metals could be related to the partial reduction of TiO_2 . It means that some oxygen from the $\text{TiO}(\delta+)$ lattice was replaced by Pd, as demonstrated by Wang *et al.* (2021). In this sense, assuming the form of a reduced titania state, a promoting effect of TiO_2 can be expected in nitrate reduction (Krawczyk *et al.* 2011). The authors also found, after 1 h of reaction, the presence of trace amounts of Pd in the reaction solution when the catalyst was prepared with Al_2O_3 and SiO_2 as support, while no Pd was detected in the reaction medium when TiO_2 was used.

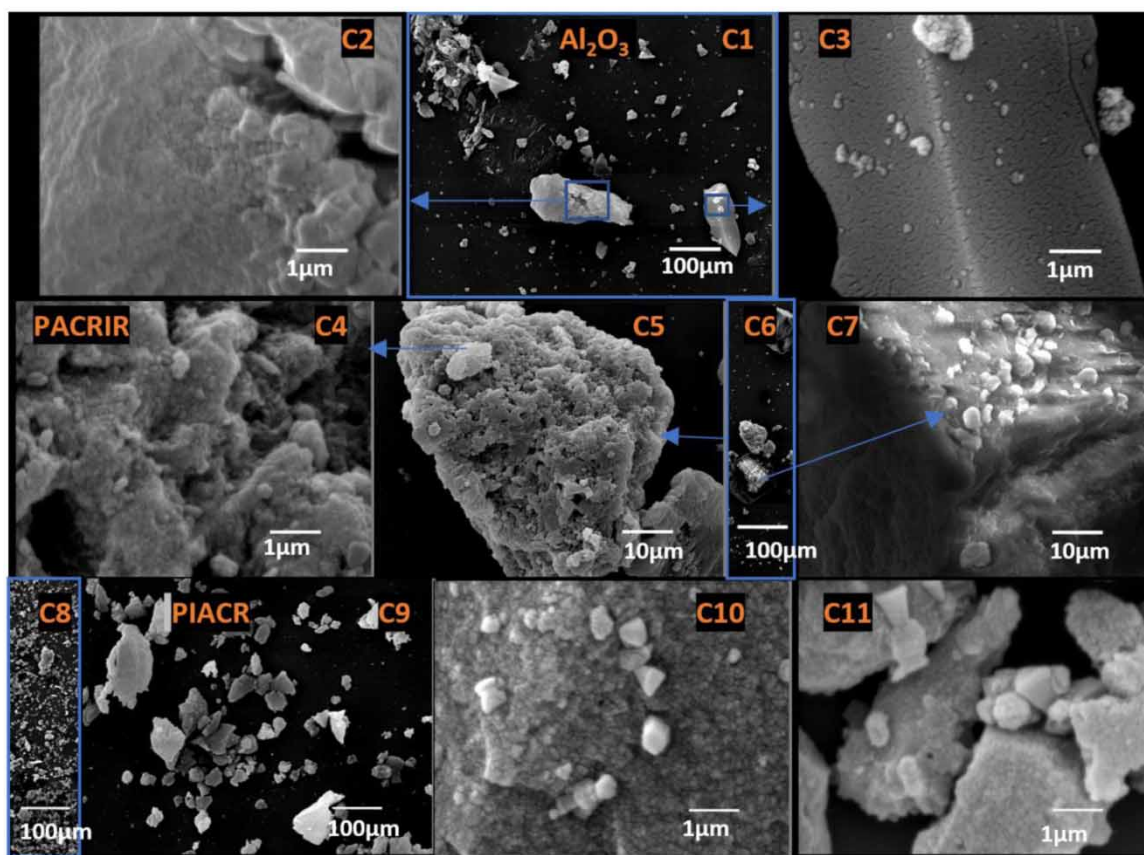


Figure 5 | SEM micrographs of γ - Al_2O_3 (C1–C3), PACRIR (C4–C7), and PIACR (C8–C11).

3.2. Nitrate removal evaluation

3.2.1. Alumina-supported catalysts

Figure 6 shows the N-compound concentration as a function of time over the alumina-supported catalysts. These profiles give insight into the catalytic performance of the alumina-supported catalysts on nitrate removal.

All the prepared Al_2O_3 -supported catalysts resulted in being active in nitrate conversion (Figure 6(a)). Total conversions and conversions close to 100% were obtained, with PIACR being the catalyst with the best catalytic activity. The best catalytic activity is defined as the one which reaches the highest conversion and selectivity in the lowest time. When the catalysts were compared at the same conversion (90%), PIACR was the one that obtained the best selectivity at the lowest time with the same conversion (see Table 2). In the wet co-impregnation method, Pd and In cations were atomically mixed and their dispersion over the support was extensive before being calcinated (Frei *et al.* (2019)). With this calcination step: (1) Pd and In fixed to the support and between them, a metal/metal oxide interaction (MMOI) was produced (Jia *et al.* 2017); (2) then, after reduction, the metallic promoted particles could react with the nitrate to convert it in nitrite; (3) nitrite reacted with the hydrogen adsorbed on Pd atoms and continued the reduction reaction to produce nitrogen or ammonia. Additionally, this behavior was reported and associated with the positive charge developed by the alumina surface, which introduced an attractive force between the positive alumina surface and the negative nitrate and nitrite ions leading by opposite charges (alumina isoelectric point = 8, at reaction pH = 5, the alumina surface is positive) (Marchesini *et al.* 2012).

Each reaction will always preponderate depending on the control of the reaction media. Schematically, the reaction followed the mechanism presented above (Equation (1)–(3)). In the Supplementary Material (Equations S1–S4), the mechanism taking into consideration the active sites and the physisorption is described. The $\text{NO}_2(\text{ads})$ reacted with the $\text{H}(\text{ads})$ and produced $\text{NO}(\text{ads})$, which was considered the clue particle (Clark *et al.* 2020). This $\text{NO}(\text{ads})$ could dissociate and form N_2 when joined with another $\text{NO}(\text{ads})$, or this $\text{NO}(\text{ads})$ could be hydrogenated to form $\text{N}(\text{ads})$, $\text{NH}(\text{ads})$, $\text{NH}_2(\text{ads})$,

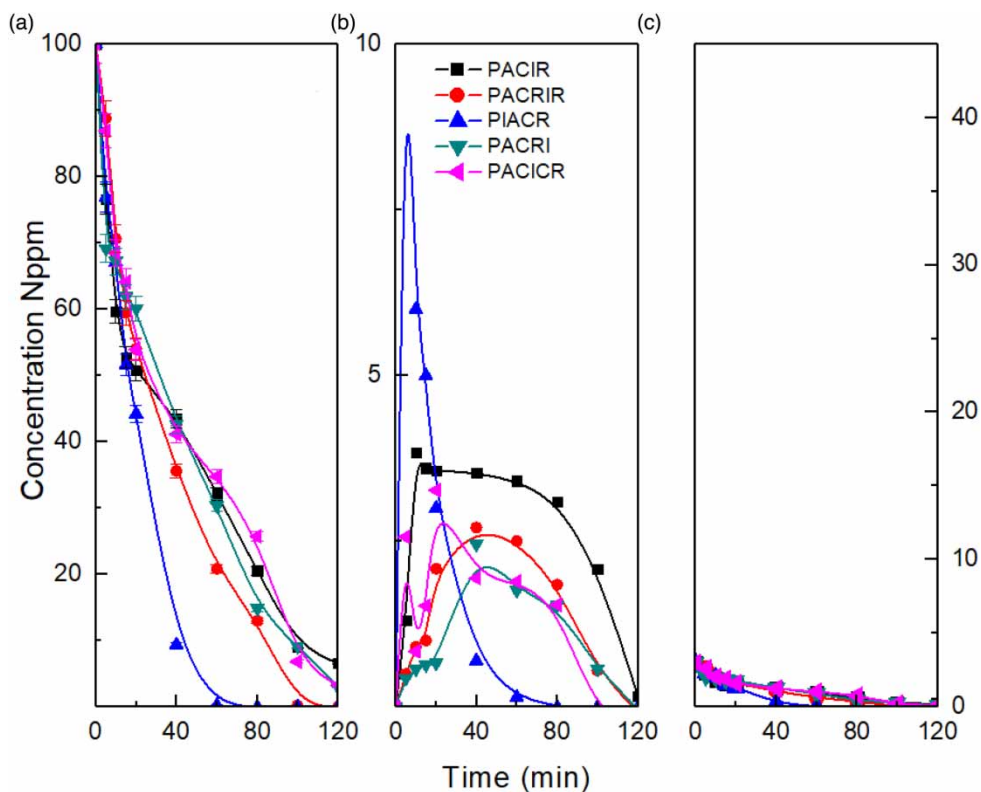


Figure 6 | Evaluation of Pd:In catalysts supported on Al_2O_3 . Concentrations of N-compounds as a function of the reaction time: (a) nitrate; (b) nitrite; and (c) ammonium.

NH_3 , or could couple to form N_2O_4 . For Equation (1), the initial rate expression was a pseudo-first-order reaction:

$$-\frac{dC_{\text{NO}_3^-}^t}{dt} = v_i = k' C_{\text{NO}_3^-}^t \quad (6)$$

Table 2 | Selectivities of those catalysts that achieved 90% nitrate reduction

Catalyst	t(min) X = 90%	S[NO ₂] (%)	S[NH ₄ ⁺] (%)	S[N ₂] (%)	v _i (ppm/min)	X (%) at 120 min
PACIR	100	2.3	13.7	84.0	4.9	94.6
PACRIR	84	1.2	4.4	94.4	2.3	100
PIACR	44	0.9	20.8	78.3	4.4	100
PACRI	96	0.9	11.6	87.5	5.2	98.5
PACICR	98	0.3	13.0	86.7	2.8	98.1
PIACR(H ₂) ^a	30	2.2	22.2	75.6	7.1	100
PTCRIR	96	0.6	40.4	59.0	7.8	97.8
PTICR	97	0.7	24.2	75.1	5.5	80.1
PTCRI	83	0.6	17.0	82.4	4.2	100
PTCICR	100	0.3	37.9	61.8	4.2	98.8
PITCR(H ₂) ^b	35	2.7	16.1	81.2	3.5	100

^aMarchesini *et al.* (2008a).

^bMarchesini (2008).

This expression represents an apparent initial velocity, where k' is the reaction constant and it includes the reductant agent concentration due to the H_2 in excess. The catalyst's behavior was not affected by reaction products when it was calculated at less than 5%–10% nitrate conversion, and it was possible to compare the initial rate of each catalyst as a representation of the maximal catalytic activity (Hall *et al.* 1976; Casado *et al.* 1986). The catalyst initial rate, calculated v_1 (ppm/min), can be observed in Table 2.

In addition, it was reported that the catalytic performance of Pd,In/Al₂O₃ systems in nitrate and nitrite reduction was influenced by the formation of the intermetallic phase and/or the increase in indium surface concentrations in those bimetallic systems (Krawczyk *et al.* 2011). Moreover, it is widely reported that the selectivity to N₂ is higher for catalysts with lower dispersion (Yoshinaga *et al.* 2002; Gauthard *et al.* 2003; Garron *et al.* 2005; Zhang *et al.* 2008a). The lowest availability of active sites saturated with hydrogen avoided the over-reduction of nitrites and increased the selectivity to nitrogen (Tokazhanov *et al.* 2020).

Regarding nitrite production, the highest nitrite concentration was detected (Figure 6(b)) at the beginning of the reaction with PIACR, the most active catalyst. The same behavior was observed with the formation of ammonium (Figure 6(c)), where the PIACR catalyst produced the largest amount of this reaction by-product in line with our previous work (Marchesini *et al.* 2012). It was reported that the amounts of NH₄⁺ produced depended on the mutual interactions between Pd and In and also on the porosity of the support (Krawczyk *et al.* 2011). A mutual interaction promoted a high recuperation of the reduced active sites which participated in the over-reduction from nitrite to ammonia, and porosity was involved in the generation of microenvironments which were inaccessible for the buffering system to neutralize, which increased the generation of ammonia pathway by-products. This behavior could be additionally related to the fact that Pd and In were co-impregnated, inducing a higher metal–metal interaction as revealed by the SEM-EDS analysis since the support used in all catalysts was the same (Figure 6). In terms of composition, particles with Pd and In were more active for nitrate conversion. However, there was more H-Pd availability when the surface was richer in Pd, allowing over-reduction. This situation favored reduction and higher selectivity to ammonia. Porosity had a great effect on the reaction because the system was not able to buffer the OH generated by each nitrate converted, so the environment near the active site became an alkaline region. It was reported that the alkaline pH promoted the increase of ammonia as the final product (Santos *et al.* 2020).

Nevertheless, no linear trend was observed between catalytic activity and ammonium production. For example, the second most active catalyst supported on alumina was PACRIR, but it produced the least amount of ammonium at the end of the reaction. There is an intense growth in knowledge about this reaction pathway (Sanchis *et al.* 2022). Since nitrate is converted to nitrite through a very quick reaction, it is necessary to control the average pH and the availability of H adatoms as quickly as possible. There was an exquisite balance between these variables that favored one or the other reaction pathway. In the case of the PACRIR catalyst, the Pd was calcinated and then reduced before depositing In, so the interaction generated between Pd and In was probably more intense. As mentioned above, the presence of In slightly prevented Pd from dissociatively adsorbing H, so the reaction occurred as quickly as possible, but there was no excess of H adatoms to over-reduce NO(ads) and to generate more ammonia.

However, it is important to take into account that the nitrate reduction rate and selectivity toward final products were affected by the dispersion of particles on the support, the size of the particles, and the formation of agglomerates. Dispersion and size directly affected activity and selectivity. Guo *et al.* (2018) found that at a low In loading, the element remained dispersed and in the metallic form, but In particles must be in contact with Pd to produce two types of sites with two different roles: (1) adsorb nitrate and (2) reduce nitrate. The role of Pd sites is to regenerate the In sites oxidated during nitrate reduction. Consequently, large In particles (due to low dispersion or agglomeration) block the Pd sites from dissociatively adsorbing H₂, and this leads to a lower reaction rate. In the opposite case, when PdH is abundant, over-reduction is predominant and selectivity leads to ammonia generation.

These factors, in turn, depend on the preparation method and the metal loading (Martínez *et al.* 2017). On the other hand, Pd particle size considerably affects the selectivity to N₂, with better selectivity being obtained in the presence of metallic agglomerates (Yoshinaga *et al.* 2002; Garron *et al.* 2005; Zhang *et al.* 2008; Soares *et al.* 2021). Marchesini (2008) and Zhang *et al.* (2008) found that selectivity was greatly correlated to the size of active metal particles. Pd–In particles tended to agglomerate in reducing aqueous media, and bigger particles increased the N(ads)/H(ads) ratio, so it is more possible that two N(ads) find each other generating N₂, resulting in a better selectivity (see the mechanism in the Supplementary Material, Equations S1–S5).

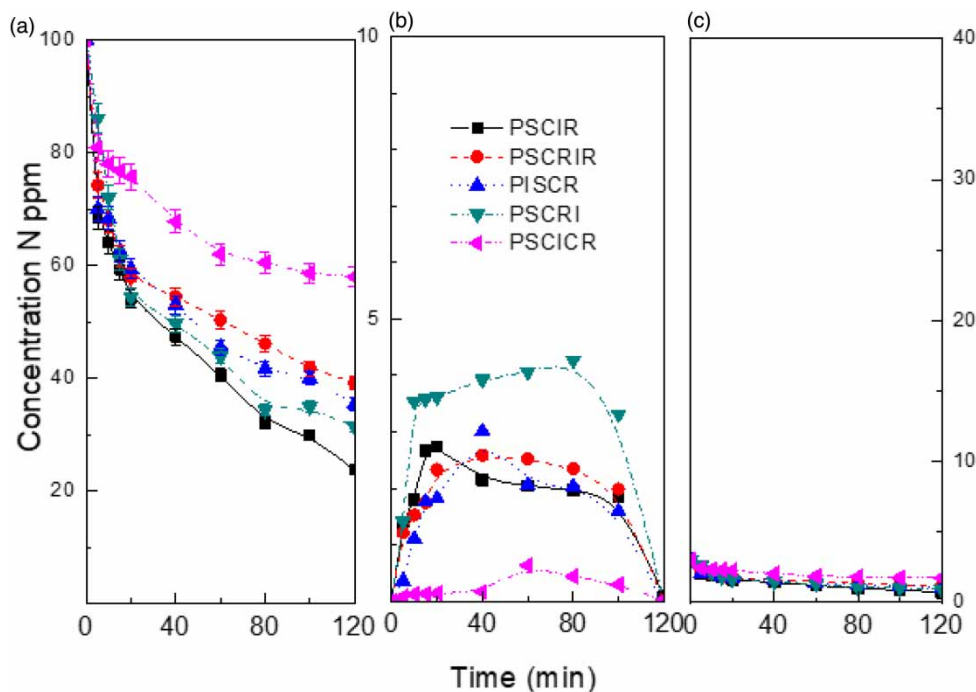


Figure 7 | Evaluation of Pd:In catalysts supported on SiO₂. Concentrations of N-compounds as a function of the reaction time: (a) nitrate; (b) nitrite; and (c) ammonium.

3.2.2. Silica-supported catalysts

Nitrate reduction employing SiO₂-supported catalysts is summarized in Figure 7. None of the catalysts showed 100% nitrate conversion. The catalyst that achieved the highest conversion at 120 min was PSCIR (76.4%), and the one that converted the least amount of nitrate was PSCICR (42.1%). Despite having a high surface area, catalysts supported on silica showed a lower conversion than those supported on alumina. The lower catalytic activity might be related to the higher electrostatic repulsion in the reaction medium since the catalysts were negatively charged on the surface at the working pH, which was superior to the isoelectric point of this supported catalyst (see Table S3 in the Supplementary Material), considering that the silica isoelectric point range is 2–4 (Munnik *et al.* 2015). Furthermore, a Pd:In ratio of 2 was observed for this best-performing catalyst (PSCIR), inferring that much of the Pd could be, in bulk, inaccessible for nitrate reduction.

3.2.3. Titania-supported catalysts

Figure 8 shows the catalytic performance of catalysts supported on TiO₂ for nitrate removal. Figure 8(a) shows that catalysts supported on TiO₂ obtain total conversion, except for the PTCIR catalyst, which obtained 80.1% of nitrate elimination. In Figure 8(b), the formation of nitrite can be observed, just as in the supports presented previously. However, the maximum concentration detected (PTCRI, 2 ppm, $t = 20$ min) was lower than the maximum concentrations detected for alumina (PIACR, 8 ppm, $t = 10$ min) and silica (PSCRI, 4.2 ppm, $t = 80$ min), which may indicate a higher activity in the second reaction step, in comparison with the previously mentioned supports. The high rate of disappearance of nitrite was indicative of the high density of Pd-H sites, which could rapidly reduce this ion, and as soon as the nitrite was reduced, it was delivered to the reaction media, allowing the exposed Pd sites to adsorb H and continue with the reaction (Zhang *et al.* 2008). This higher nitrite reduction activity also reflected a higher formation of ammonium as a product, compared with the previous supports.

Regarding the support structure in TiO₂, Kim *et al.* (2013) prepared 2.5 wt.% Pd/1 wt.% Cu bimetallic catalysts supported on TiO₂ with different anatase-/rutile-phase compositions for the reduction of nitrate in water. Catalysts containing a higher anatase-phase composition were shown to have superior catalytic performance. The maximum nitrate conversion obtained was 100% in 40 min of reaction, with the catalyst with the highest content of the anatase phase (98%). In general, the TiO₂-supported catalysts prepared in this work obtained better results than the Pd,Cu/TiO₂ reported by Kim *et al.* (2013), with some of them reaching total conversion. It is important to highlight that this author used an almost twice-higher metallic

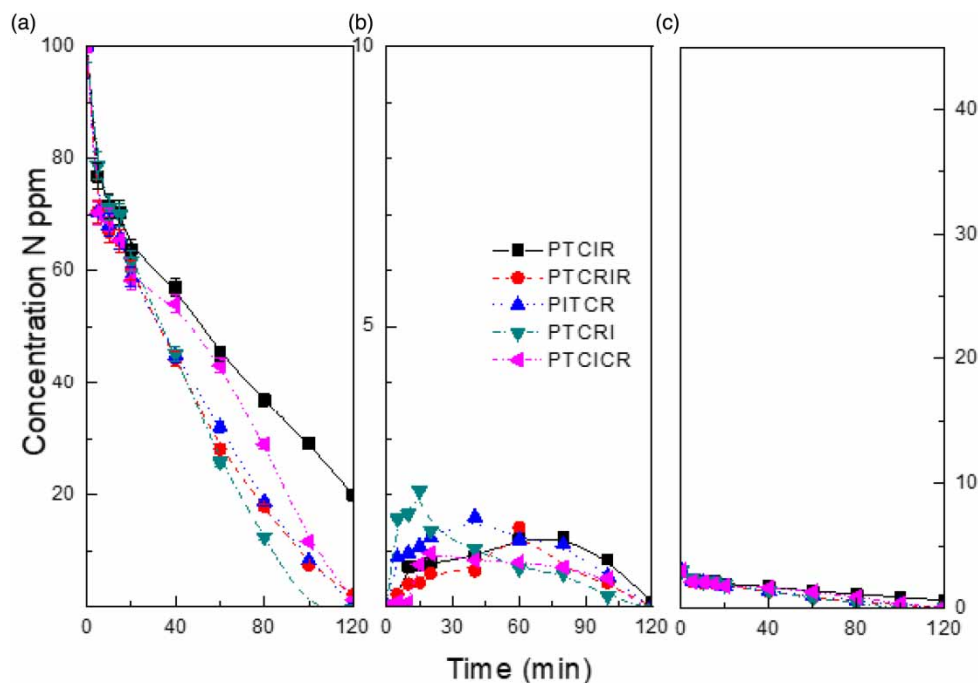


Figure 8 | Evaluation of Pd:In catalysts supported on TiO_2 . Concentrations of N-compounds as a function of the reaction time: (a) nitrate; (b) nitrite; and (c) ammonium.

concentration (2.5:1 wt.% Pd:Cu), so our catalyst resulted in being more sustainable. The conditions slightly favored our material since it had a lower metal loading (1:0.25 wt.% Pd:In), starting with a higher contaminant concentration (7.4 mM) and then obtaining total conversion and similar selectivity at the same time.

Thus, according to the results obtained, we can conclude that the most active catalysts in the catalytic reduction of nitrate were those prepared on alumina, followed by titania and then by the least active one supported on silica. The results obtained showed that nitrites were present in high concentrations in the reaction mixture only in the initial stage of the reaction for Pd, In/ Al_2O_3 and Pd, In/ SiO_2 catalysts. A lower concentration of this product was not observed when using Pd, In/ TiO_2 .

On the other hand, taking into account the specific surface of supports used (Al_2O_3 , SiO_2 , and TiO_2), it is widely known that the order in increasing values of the surface area is $\text{TiO}_2 > \text{Al}_2\text{O}_3 > \text{SiO}_2$. However, the catalytic performances found resulted in the following increasing order of activity: $\text{Al}_2\text{O}_3 > \text{TiO}_2 > \text{SiO}_2$. Therefore, we can assume that the catalytic performance was mostly affected by the type of interaction between the active phases (Pd and In) and between the active phases and the support (Sanchis *et al.* 2022).

It is important to consider that generally, supports that can disperse the In_2O_3 aggregates with high In stabilization could give an increase to active catalytic systems. In this work, alumina and titania supports of the catalysts with the highest catalytic activity have been reported as supports with high In dispersion. It is known that a balance between basic and acidic sites on the support surface plays an important role in the stabilization of In_2O_3 particles. Silica is a very low acid support which favors the agglomeration of the In particles (Gervasini *et al.* 2006), decreasing the contact with Pd which is essential for the development of the reaction. This behavior was observed by SEM-EDS analysis. Comparing the distribution of In in the catalysts prepared on SiO_2 (Figures S1 and S2) with those supported on Al_2O_3 (Figures S4–S8), it can be observed that alumina significantly favored the distribution of In on its surface, while silica generated In agglomerates and a less homogeneous distribution.

3.3. Selectivity of the most active catalysts

Table 2 summarizes the selectivities toward nitrite, nitrogen gas, and ammonium with those catalysts that reached 90% conversion. Also, a comparison with the three types of supports for the catalysts used in this work, in the same nitrate conversion, is shown in the Supplementary Material (Table S2).

Firstly, it is important to mention that the catalysts that promoted catalysts with a catalytic activity greater than 90% were those supported by Al_2O_3 and TiO_2 . Regarding N_2 selectivity, the most efficient for the alumina group was PACRIR, with 94.4% selectivity to N_2 . Even so, the Pd 1%, In 0.25% catalysts already reported in the literature showed lower selectivity to N_2 at 90% conversion.

On the other hand, the ammonium selectivity, which is the main drawback in this process, of the alumina group was between 1.6% and 16% at the same nitrate conversion (42%), the PACRIR catalyst being the one that achieved the lowest ammonium selectivity (see Table S2). The group of catalysts supported on SiO_2 presented ammonium selectivity in the range of 11.2%–17.1%, and the catalysts supported on TiO_2 presented higher ammonium selectivity values between 7.1% and 32.1%.

In a previous work (Marchesini *et al.* 2008b), a selectivity to N_2 of 75.6% was obtained by achieving 90% nitrate elimination. In that work, the reduction step during the synthesis was carried out with H_2 at 450 °C and the active phase was added in a single impregnation, comparable to the PIACR of this work ($S(\text{N}_2) = 78.3\%$). Since the operating conditions were the same, the main changes involved the interactions between the active phase and support during the synthesis. On the one hand, the results of the present work may show an advantage in using liquid-phase reduction compared with gas-phase reduction. Moreover, the addition of Pd and In in different steps represented a distribution of the particles on the surface in a way that favored the selectivity toward N_2 . In this sense, it is reasonable that the PIACR catalyst presented the lowest selectivity to N_2 since it showed good distribution of Pd and In on the support surface, and generally, the selectivity to N_2 was higher for catalysts with lower dispersion (Yoshinaga *et al.* 2002; Garron *et al.* 2005; Zhang *et al.* 2008; Soares *et al.* 2021).

Regarding TiO_2 catalysts, the best selectivity to N_2 (82.4%) was obtained with PTCRI. The catalysts supported on TiO_2 showed a higher selectivity to NH_4^+ compared with alumina and PACRIR (17.0% and 4.4%, respectively), indicating that the interaction between the active phase and support was different. In the case of TiO_2 , as mentioned in the discussion of the SEM-EDS results, there may be more formation of Pd species with low coordination numbers, i.e., corner and edge positions due to the strong interaction of Pd with the support (Sá & Vinek 2005). These terminations have a higher hydrogenation capacity, facilitating the reduction of nitrite to NH_4^+ at these sites. These results are contrary to those obtained by Krawczyk *et al.* (2011), where the Pd5%/In2%/TiO₂ catalysts with the lowest ammonium production were those supported on titania, compared with those supported on alumina, and at the same time showed the highest selectivity to N_2 . The physicochemical properties of TiO_2 in Krawczyk *et al.* (2011) were different. It had a range of pore diameters of 100–300 Å, so the capacity to neutralize the OH produced during the nitrate reduction was higher than the one from this work. In this sense, the local pH developed inside the pores must be higher than the one produced on titania in Krawczyk *et al.* (2011).

Regarding the initial rates, no direct connection was found with the Pd content (see Table S4 in the Supplementary Material), indicating that other factors had a greater impact on this variable. As for alumina-supported catalysts, those in which In was added at the end (PACRI) showed a higher v_i than the same catalyst in which reduction took place after the addition of In (PACRIR). Among these catalysts, reduction after In deposition induced a small surface loss of Pd (Table 1) compared with the catalyst in which no reduction step was performed after In deposition (see Table S2).

Conversely, PTCRI presented a lower initial rate than PTCRIR with the TiO_2 support. Thus, although both catalysts showed similar values of N_2 selectivity and nitrate conversion at 120 min, the fact that there was a higher surface Pd (PACRI) led to higher conversion at the beginning of the reaction.

4. CONCLUSIONS

(Pd,In)-based catalysts deposited by wet impregnation onto alumina (Al_2O_3), silica (SiO_2), and titania (TiO_2) were prepared and evaluated for nitrate removal from water to study the influence of supports on catalytic performance and selectivity. In comparison with Al_2O_3 and SiO_2 , a strong interaction between the TiO_2 support and its active phase was observed. Catalysts supported onto Al_2O_3 and SiO_2 showed a weaker MSI which favored N_2 selectivity and less retention of Pd and In in the bulk. The alumina-supported catalysts generally showed better catalytic activity, followed by the titanium-oxide-supported catalysts. Different sequential processes were applied to obtain catalysts that were more stable, active, and selective to nitrogens. The PACRIR catalyst, whose process includes the deposition of Pd over alumina + calcination + reduction + In impregnation and final reduction, was the sequence that produced the better sum of properties. The best compromise

between activity and selectivity was obtained with the alumina-supported catalyst, which is synthesized by the PACRIR method. These results suggest that bimetallic In on Pd-supported catalysts can reduce efficiently the nitrate content in water, and a sequential synthesis is a powerful tool for improving this capability and increasing selectivity to N₂.

ACKNOWLEDGEMENTS

The authors wish to acknowledge the financial support of FIQ-UNL, INCAPE, CONICET, ANPCyT, PICT 2019 2019-02970, CAI + D 2020 50620190100148LI, of Argentina, Red CYTED Nro. 318RT0551, CNPq and CAPES from Brazil. Thanks are also given to translator Yanina Burkett Beliz for editing the English-language manuscript.

DATA AVAILABILITY STATEMENT

All relevant data are included in the paper or its Supplementary Information.

CONFLICT OF INTEREST

The authors declare there is no conflict.

REFERENCES

- APHA/AWWA/WEF 2017 *Standard Methods for the Examination of Water and Wastewater*, 23rd edn. APHA/AWWA/WEF, Washington, DC, USA.
- Byun, M. Y., Park, D. W. & Lee, M. S. 2020 Effect of oxide supports on the activity of Pd based catalysts for furfural hydrogenation. *Catalysts* **10**, 837. <https://doi.org/10.3390/catal10080837>.
- Casado, J., Arturo Lopez-Quintela, M. & Lorenzo-Banal, F. M. 1986 The initial rate method in chemical kinetics: evaluation and experimental illustration. *J. Chem. Educ.* **63** (5), 450–452.
- Chauhan, R. & Srivastava, V. C. 2021 A suitable combination of electrodes for simultaneous reduction of nitrates and oxidation of ammonium ions in an explosive industry wastewater. *Ind. Eng. Chem. Res.* **60**, 5482–5493. <https://doi.org/10.1021/acs.iecr.1c00130>.
- Chen, P., Khetan, A., Yang, F., Migunov, V., Weide, P., Stürmer, S. P., Guo, P., Kähler, K., Xia, W., Mayer, J., Pitsch, H., Simon, U. & Muhler, M. 2017 Experimental and theoretical understanding of nitrogen-doping-induced strong metal–support interactions in Pd/TiO₂ catalysts for nitrobenzene hydrogenation. *ACS Catalysis* **7** (2), 1197–1206. <https://doi.org/10.1021/acscatal.6b02963>.
- Clark, C. A., Reddy, C. P., Xu, H., Heck, K. N., Luo, G., Senftle, T. P. & Wong, M. S. 2020 Mechanistic insights into pH-controlled nitrite reduction to ammonia and hydrazine over rhodium. *ACS Catal.* **10**, 494–509. <https://doi.org/10.1021/acscatal.9b03239>.
- Coq, B. 2000 Metal-support interaction in catalysis. In: *Metal-Ligand Interactions in Chemistry, Physics and Biology* (N. Russo & D. R. Salahub, eds), Kluwer, Dordrecht, The Netherlands, pp. 49–71. https://doi.org/10.1007/978-94-011-4245-8_5.
- Devadas, A., Vasudevan, S. & Epron, F. 2011 Nitrate reduction in water: influence of the addition of a second metal on the performances of the Pd/CeO₂ catalyst. *J. Hazard. Mater.* **185**, 1412–1417. <https://doi.org/10.1016/j.jhazmat.2010.10.063>.
- Durkin, D. P., Ye, T., Choi, J., Livi, K. J. T., De Long, H. C., Trulove, P. C., Fairbrother, D. C., Haverhals, L. M. & Shuai, D. 2018 Sustainable and scalable natural fiber welded palladium-indium catalysts for nitrate reduction. *Appl. Catal. B* **221**, 290–301. <https://doi.org/10.1016/j.apcatb.2017.09.029>.
- Fu, J., Yao, F., Xie, T., Zhong, Y., Tao, Z., Chen, S., He, L., Pi, Z., Hou, K., Wang, D., Li, X. & Yang, Q. 2021 In-situ growth of needle-like Co₃O₄ on cobalt foam as a self-supported cathode for electrochemical reduction of nitrate. *Sep. Purif. Technol.* **276**, 119329. <https://doi.org/10.1016/j.seppur.2021.119329>.
- Fu, W., Hu, Z., Zheng, Y., Su, P., Zhang, Q., Jiao, Y. & Zhou, M. 2022 Tuning mobility of intermediate and electron transfer to enhance electrochemical reduction of nitrate to ammonia on Cu₂O/Cu interface. *Chem. Eng. J.* **433**, 133680. <https://doi.org/10.1016/j.cej.2021.133680>.
- Fuentes, C. A. B. & Hwang, Y. 2021 Catalytic reduction of nitrate in reverse osmosis concentrate by using Pd-Cu/activated carbon felt. *Energy Environ.* **32**, 152–167. <https://doi.org/10.1177/0958305X20923115>.
- Frei, M. S., Mondelli, C., García-Muelas, R., Kley, K. S., Puértolas, B., López, N., Safonova, O. V., Stewart, J. A., Ferré, D. C. & Pérez-Ramírez, J. 2019 Atomic-scale engineering of indium oxide promotion by palladium for methanol production via CO₂ hydrogenation. *Nature Communications* **10** (1), 3377. <https://doi.org/10.1038/s41467-019-11349-9>.
- García-Segura, S., Lanzarini-Lopes, M., Hristovski, K. & Westerhoff, P. 2018 Electrocatalytic reduction of nitrate: fundamentals to full-scale water treatment applications. *Appl. Catal. B* **236**, 546–568. <https://doi.org/10.1016/j.apcatb.2018.05.041>.
- Garron, A., Lázár, K. & Epron, F. 2005 Effect of the support on tin distribution in Pd–Sn/Al₂O₃ and Pd–Sn/SiO₂ catalysts for application in water denitration. *Appl. Catal. B* **59**, 57–69. [https://doi.org/10.1016/S0021-9517\(03\)00252-5](https://doi.org/10.1016/S0021-9517(03)00252-5).
- Gauthard, F., Epron, F. & Barbier, J. 2003 Palladium and platinum-based catalysts in the catalytic reduction of nitrate in water: effect of copper, silver, or gold addition. *J. Catal.* **220**, 182–191. [https://doi.org/10.1016/S0021-9517\(03\)00252-5](https://doi.org/10.1016/S0021-9517(03)00252-5).
- Gervasini, A., Perdigon-Melon, J. A., Guimon, C. & Auroux, A. 2006 An in-depth study of supported In₂O₃ catalysts for the selective catalytic reduction of NO_x: the influence of the oxide support. *J. Phys. Chem. B* **110**, 240–249. <https://doi.org/10.1021/jp0532824>.

- Guo, S., Heck, K., Kasiraju, S., Qian, H., Zhao, Z., Grabow, L. C., Miller, J. T. & Wong, M. S. 2018 Insights into nitrate reduction over indium-decorated palladium nanoparticle catalysts. *ACS Catal.* **8** (1), 503–515. doi:10.1021/acscatal.7b01371.
- Hall, K. J., Quickenden, T. I. & Watts, D. W. 1976 Rate constants from initial concentration data. *J. Chem. Educ.* **53** (8), 493–494.
- Hamid, S., Niaz, Y., Bae, S. & Lee, W. 2020 Support induced influence on the reactivity and selectivity of nitrate reduction by Sn-Pd bimetallic catalysts. *J. Environ. Chem. Eng.* **8**, 103754. https://doi.org/10.1016/j.jece.2020.103754.
- Hurtado-Martinez, M., Muñoz-Palazon, B., Robles-Arenas, V. M., Gonzalez-Martinez, A. & Gonzalez-Lopez, J. 2021 Biological nitrate removal from groundwater by an aerobic granular technology to supply drinking water at pilot-scale. *J. Water Process. Eng.* **40**, 101786. https://doi.org/10.1016/j.jpwe.2020.101786.
- Imura, Y., Tsujimoto, K., Morita, C. & Kawai, T. 2014 Preparation and catalytic activity of Pd and bimetallic Pd–Ni nanowires. *Langmuir* **30**, 5026–5030. https://doi.org/10.1021/la500811n.
- Jia, Q., Ghoshal, S., Li, J., Liang, W., Meng, G., Che, H., Zhang, S., Ma, Z. & Mukerjee, S. 2017 Metal and metal oxide interactions and their catalytic consequences for oxygen reduction reaction. *J. Am. Chem. Soc.* **139**, 7893–7903. https://doi.org/10.1021/jacs.7b02378.
- Kiani, A., Sharafi, K., Omer, A. K., Matin, B. K., Davoodi, R., Mansouri, B., Sharafi, H., Soleimani, H., Massahi, T. & Ahmadi, E. 2022 Accumulation and human health risk assessment of nitrate in vegetables irrigated with different irrigation water sources – transfer evaluation of nitrate from soil to vegetables. *Environ. Res.* **205**, 112527. https://doi.org/10.1016/j.envres.2021.112527.
- Kim, M., Chung, S., Yoo, C., Lee, M., Cho, I., Lee, D. & Lee, K. 2013 Catalytic reduction of nitrate in water over Pd–Cu/TiO₂ catalyst: effect of the strong metal-support interaction (SMSI) on the catalytic activity. *Appl. Catal. B* **142–143**, 354–361. https://doi.org/10.1016/j.apcatb.2013.05.033.
- Krawczyk, N., Karski, S. & Witońska, I. 2011 The effect of support porosity on the selectivity of Pd–In/support catalysts in nitrate reduction. *React. Kinet. Mech. Catal.* **103**, 311–323. https://doi.org/10.1007/s1144-011-0321-4.
- Li, H., Guo, S., Shin, K., Wong, M. S. & Henkelman, G. 2019 Design of a Pd–Au nitrite reduction catalyst by identifying and optimizing active ensembles. *ACS Catal.* **9**, 7957–7966. https://doi.org/10.1021/acscatal.9b02182.
- Li, Z., Zhang, M., Dong, X., Ji, S., Zhang, L., Leng, L., Li, H., Horton, J. H., Xu, Q. & Zhu, J. 2022 Strong electronic interaction of indium oxide with palladium single atoms induced by quenching toward enhanced hydrogenation of nitrobenzene. *Appl. Catal. B* **313**, 121462. doi:10.1016/j.apcatb.2022.121462.
- Liu, Y., Zhang, X. & Wang, J. 2022 A critical review of various adsorbents for selective removal of nitrate from water: structure, performance and mechanism. *Chemosphere* **291**, 132728. https://doi.org/10.1016/j.chemosphere.2021.132728.
- Lou, Y., Xu, J., Zhang, Y., Pan, C., Dong, Y. & Zhu, Y. 2020 Metal-support interaction for heterogeneous catalysis: from nanoparticles to single atoms. *Mater. Today Nano* **12**, 100093. https://doi.org/10.1016/j.mtnano.2020.100093.
- Lv, X., Peng, H., Wang, X., Hu, L., Peng, M., Liu, Z. & Jiang, G. 2022 Nitrate reduction by nanoscale zero valent iron (nFe⁰)-based systems: mechanism, reaction pathway and strategy for enhanced N₂ formation. *Chem. Eng. J.* **430**, 133133. https://doi.org/10.1016/j.cej.2021.133133.
- Marchesini, F. A. 2008 *Tecnologías Catalíticas para el tratamiento de aguas. Eliminación de Nitratos y Nitritos en agua utilizando catalizadores bimetalicos*. PhD thesis, Universidad Nacional del Litoral, Santa Fe, Argentina.
- Marchesini, F. A., Irusta, S., Querini, C. & Miró, E. 2008a Spectroscopic and catalytic characterization of Pd–In and Pt–In supported on Al₂O₃ and SiO₂, active catalysts for nitrate hydrogenation. *Appl. Catal. A Gen.* **348**, 60–70. https://doi.org/10.1016/j.apcata.2008.06.026.
- Marchesini, F. A., Irusta, S., Querini, C. & Miró, E. 2008b Nitrate hydrogenation over Pt,In/Al₂O₃ and Pt,In/SiO₂. Effect of aqueous media and catalyst surface properties upon the catalytic activity. *Catal. Commun.* **9**, 1021–1026. https://doi.org/10.1016/j.catcom.2007.09.037.
- Marchesini, F. A., Picard, N. & Miró, E. E. 2012 Study of the interactions of Pd,In with SiO₂ and Al₂O₃ mixed supports as catalysts for the hydrogenation of nitrates in water. *Catal. Commun.* **21**, 9–15. https://doi.org/10.1016/j.catcom.2012.01.015.
- Martínez, J., Ortiz, A. & Ortiz, I. 2017 State-of-the-art and perspectives of the catalytic and electrocatalytic reduction of aqueous nitrates. *Appl. Catal. B* **207**, 42–59. https://doi.org/10.1016/j.apcatb.2017.02.016.
- Munnik, P., de Jongh, P. E. & de Jong, K. P. 2015 Recent developments in the synthesis of supported catalysts. *Chem. Rev.* **115**, 6687–6718. https://doi.org/10.1021/cr500486u.
- Pang, Y. & Wang, J. 2021 Various electron donors for biological nitrate removal: a review. *Sci. Total Environ.* **794**, 148699. https://doi.org/10.1016/j.scitotenv.2021.148699.
- Park, J., Hwang, Y. & Bae, S. 2019 Nitrate reduction on surface of Pd/Sn catalysts supported by coal fly ash-derived zeolites. *J. Hazard. Mater.* **374**, 309–318. https://doi.org/10.1016/j.jhazmat.2019.04.051.
- Qasemi, M., Farhang, M., Morovati, M., Mahmoudi, M., Ebrahimi, S., Abedi, A., Bagheri, J., Zarei, A., Bazeli, J., Afsharnia, M., Ghalehaskar, S. & Ghaderpoury, A. 2022 Investigation of potential human health risks from fluoride and nitrate via water consumption in Sabzevar, Iran. *Int. J. Environ. Anal. Chem.* **102**, 307–318. https://doi.org/10.1080/03067319.2020.1720668.
- Ramalingam, S. & Subramania, A. 2021 Effective removal of nitrates from the drinking water by chemical and electrochemical methods. *Engineered Science* **15**, 80–88.
- Ren, Y. W., Guo, Y., Zhao, D. Y., Wang, H. L., Wang, N., Jiang, W. W., Liu, S. M., Liu, C. Q., Ding, W. Y. & Zhang, Z. H. 2022 Preparation and characterization of rutile TiO₂ nanoparticles by HCl-water volatilization-assisted precipitation method. *J. Cryst. Growth* **577**, 126410. https://doi.org/10.1016/j.jcrysgro.2021.126410.

- Sá, J. & Vinek, H. 2005 Catalytic hydrogenation of nitrates in water over a bimetallic catalyst. *Appl. Catal. B* **57**, 247–256. <https://doi.org/10.1016/j.apcatb.2004.10.019>.
- Sanchis, I., Díaz, E., Pizarro, A. H., Rodríguez, J. J. & Mohedano, A. F. 2021 Effect of water composition on catalytic reduction of nitrate. *Sep. Purif. Technol.* **255**, 117766. <https://doi.org/10.1016/j.seppur.2020.117766>.
- Sanchis, I., Diaz, E., Pizarro, A. H., Rodriguez, J. J. & Mohedano, A. F. 2022 Nitrate reduction with bimetallic catalysts. A stability-addressed overview. *Sep. Purif. Technol.* **290**, 120750. doi.org/10.1016/j.seppur.2022.120750.
- Santos, A. S. G. G., Restivo, J., Orge, C. A., Pereira, M. F. R. & Soares, O. S. G. P. 2020 Nitrate catalytic reduction over bimetallic catalysts: catalyst optimization. *C* **6**, 78. <https://doi.org/10.3390/c6040078>.
- Scholes, R. C., Vega, M. A., Sharp, J. O. & Sedlak, D. L. 2021 Nitrate removal from reverse osmosis concentrate in pilot-scale open-water unit process wetlands. *Environ. Sci. Water Res. Technol.* **7**, 650–661. <https://doi.org/10.1039/d0ew00911c>.
- Searle, P. L. 1984 The Berthelot or indophenol reaction and its use in the analytical chemistry of nitrogen: a review. *Analyst* **109**, 549–568.
- Shen, Z., Peng, G., Gao, Y. & Shi, J. 2021 Pd–In bimetallic nanoparticles supported on chelating resin for nitrate removal from water: high efficiency and low NH_4^+ selectivity. *Environ. Sci. Water Res. Technol.* **7**, 1078–1089. <https://doi.org/10.1039/d1ew00028d>.
- Shi, X., Zhang, Y., Liu, X., Jin, H., Lv, H., He, S., Hao, H. & Li, C. 2019 A mild in-situ method to construct Fe-doped cauliflower-like rutile TiO_2 photocatalysts for degradation of organic dye in wastewater. *Catalysts* **9**, 426.
- Singh, S., Anil, A. G., Kumar, V., Kapoor, D., Subramanian, S., Singh, J. & Ramamurthy, P. C. 2022 Nitrates in the environment: a critical review of their distribution, sensing techniques, ecological effects and remediation. *Chemosphere* **287**, 131996. <https://doi.org/10.1016/j.chemosphere.2021.131996>.
- Soares, O. S. G. P., Órfão, J. J. M. & Pereira, M. F. R. 2011 Nitrate reduction in water catalysed by Pd–Cu on different supports. *Desalination* **279**, 367–374. <https://doi.org/10.1016/j.desal.2011.06.037>.
- Soares, O. S. G. P., Jardim, E. O., Ramos-Fernandez E, V., Villora-Picó, J. J., Pastor-Blas, M. M., Silvestre-Albero, J., Órfão, J. J. M., Pereira, M. F. R. & Sepulvéda-Escribano, A. 2021 Highly N_2 -selective activated carbon-supported Pt–In catalysts for the reduction of nitrites in water. *Front. Chem.* **9**, 733881. <https://doi.org/10.3389/fchem.2021.733881>.
- Tokazhanov, G., Ramazanov, E., Hamid, S., Bae, S. & Lee, W. 2020 Advances in the catalytic reduction of nitrate by metallic catalysts for high efficiency and N_2 selectivity: a review. *Chem. Eng. J.* **384**, 123252. <https://doi.org/10.1016/j.cej.2019.123252>.
- UNESCO WWAP 2019 *The United Nations World Water Development Report 2019: Leaving No One Behind*. UNESCO, Paris, France.
- Wang, J., Cheng, D., Gao, M., Li, Q., Xin, Y., Zhang, N., Zhang, Z., Yu, X., Zhao, Z. & Zhou, K. 2021 Modulation of the superficial electronic structure via metal–support interaction for H_2 evolution over Pd catalysts. *Chem. Sci.* **12**, 3245–3252. [doi:10.1039/d0sc06795d](https://doi.org/10.1039/d0sc06795d).
- Werth, C. J., Yan, C. & Troutman, J. P. 2021 Factors impeding replacement of ion exchange with (electro)catalytic treatment for nitrate removal from drinking water. *ACS ES&T Eng.* **1**, 6–20. <https://doi.org/10.1021/acsestengg.0c00076>.
- Witońska, I., Karski, S., Rogowski, J. & Krawczyk, N. 2008 The influence of interaction between palladium and indium on the activity of Pd–In/ Al_2O_3 catalysts in reduction of nitrates and nitrites. *J. Mol. Catal. A Chem.* **287**, 87–94. <https://doi.org/10.1016/j.molcata.2008.01.044>.
- Wojcieszak, R., Mateos-Blanco, R., Hauwaert, D., Carrazan, S. R. G., Gaigneaux, E. M. & Ruiz, P. 2013 Influence of the preparation method on catalytic properties of Pd/ TiO_2 catalysts in the reaction of partial oxidation of methanol. *Current Catalysis* **2** (1), 27–34. <https://doi.org/10.2174/2211544711302010006>.
- Yang, N. & Bent, S. F. 2017 Investigation of inherent differences between oxide supports in heterogeneous catalysis in the absence of structural variations. *J. Catal.* **351**, 49–58. <https://doi.org/10.1016/j.jcat.2017.04.003>.
- Yin, Y. B., Guo, S., Heck, K. N., Clark, C. A., Conrad, C. L. & Wong, M. S. 2018 Treating water by degrading oxyanions using metallic nanostructures. *ACS Sustain. Chem. Eng.* **6**, 11160–11175. <https://doi.org/10.1021/acssuschemeng.8b02070>.
- Yoshinaga, Y., Akita, T., Mikami, I. & Okuhara, T. 2002 Hydrogenation of nitrate in water to nitrogen over Pd–Cu supported on active carbon. *J. Catal.* **207**, 37–45. <https://doi.org/10.1006/jcat.2002.3529>.
- Zhang, F., Miao, S., Yang, Y., Zhang, X., Chen, J. & Guan, N. 2008 Size-dependent hydrogenation selectivity of nitrate on Pd–Cu/ TiO_2 catalysts. *J. Phys. Chem. C* **112**, 7665–7671. <https://doi.org/10.1021/jp800060g>.
- Zhao, J., Fu, J., Wang, J., Tang, K., Liu, Q. & Huang, J. 2022 Particle-size-dependent electronic metal–support interaction in Pd/ TiO_2 catalysts for selective hydrogenation of 3-nitrostyrene. *J. Phys. Chem. C* **126**, 15167–15174. <https://doi.org/10.1021/acs.jpcc.2c03945>.
- Zoppas, F. M., Bernardes, A. M., Miró, E. E. & Marchesini, F. A. 2018 Nitrate reduction of brines from water desalination plants employing a low metallic charge Pd, In catalyst and formic acid as reducing agent. *Catal. Lett.* **148**, 2572–2584. <https://doi.org/10.1007/s10562-018-2429-x>.

First received 21 June 2022; accepted in revised form 19 January 2023. Available online 31 January 2023